Semiclassical description of wavepacket dynamics in a double-minimum potential

J. Phys. B: At. Mol. Opt. Phys. 24 (1991) 5091–5102. Printed in the UK

Semiclassical description of wave packet dynamics in a double-minimum potential

W T Strunz, G Alber and J S Briggs

Fakultät für Physik, Albert-Ludwigs-Universität, Hermann-Herder-Strasse 3, D-7800 Freiburg im Breisgau, Federal Republic of Germany

Received 2 August 1991

Abstract. We study the dynamics of a vibrational molecular wave packet in single- and double-minimum potentials. A semiclassical path representation for the relevant Green function is derived in a particularly concise form by using graph theoretical concepts. Approximate analytical expressions are obtained for the two-photon transition probability which is measured in typical pump–probe experiments using two short, weak laser pulses.

1. Introduction

Laser-induced excitation of molecular wave packets by short laser pulses has become a valuable tool for studying time-dependent aspects of molecular dynamics [1]. In a typical experiment a short laser pulse excites a coherent superposition of a large number of vibrational states of an excited electronic configuration of, for example, a diatomic molecule. Thus a vibrational wave packet is prepared which represents a molecular quantum state where at each time the spread of the internuclear separation is small with respect to the size of the corresponding classically accessible region. The time evolution of this vibrational wave packet may be probed by a second short laser pulse which induces a transition to some final molecular states. According to the Franck–Condon principle this second transition usually takes place at a certain internuclear separation determined by the laser frequency. Monitoring the final state probability as a function of the time delay between both laser pulses gives a direct picture of the time evolution of such a vibrational wave packet since the transition probability is large whenever the wave packet passes the transition point.

Usually such pump–probe experiments with weak laser pulses are described theoretically by numerical solution of the Schrödinger equation which describes the dynamics of the wave packet in the excited molecular state [2]. Alternatively, the dynamics of such a wave packet may also be analysed with the help of semiclassical methods [3]. This offers the possibility of expressing the relevant quantum mechanical transition amplitude as a sum of contributions of all classical trajectories which lead from the region where the wave packet has been prepared initially to the final transition point. Such (semi-) classical path representations are particularly useful as they provide simple analytical expressions for the relevant quantum mechanical transition amplitudes and clearly exhibit the influence of laser parameters on the initial preparation process as well as the connection between the quantum mechanical wave packet propagation and the corresponding classical dynamics in the excited electronic potential.

0953-4075/91/245091+12$03.50

Motivated by recent pump–probe experiments in Na_2 [4], in this paper we study the dynamics of a vibrational molecular wave packet in a single- and double-minimum potential with the help of semiclassical methods. In section 2 we derive a semiclassical path representation for the energy-dependent Green function of a double-minimum potential. Effects of tunnelling and reflection above the potential barrier are thereby fully taken into account by uniform semiclassical approximations. For energies well above the potential barrier this Green function reduces to the corresponding result for a single-minimum potential with two turning points only. It is shown that, with the help of a suitably chosen graph and its associated adjacency matrix, this semiclassical path representation may be written in a particularly concise form. Based on these results in section 3 we derive simple, approximate analytical expressions for the two-photon-transition probability which is measured in typical pump–probe experiments.

2. Basic equations

In this section we discuss the basic equations which describe the dynamics of a laser-induced molecular wave packet in a single- and double-minimum potential. We derive a semiclassical path representation for the energy-dependent Green function of a double-minimum potential which, in the limit of high energies, reduces to the corresponding Green function of a single-minimum potential.

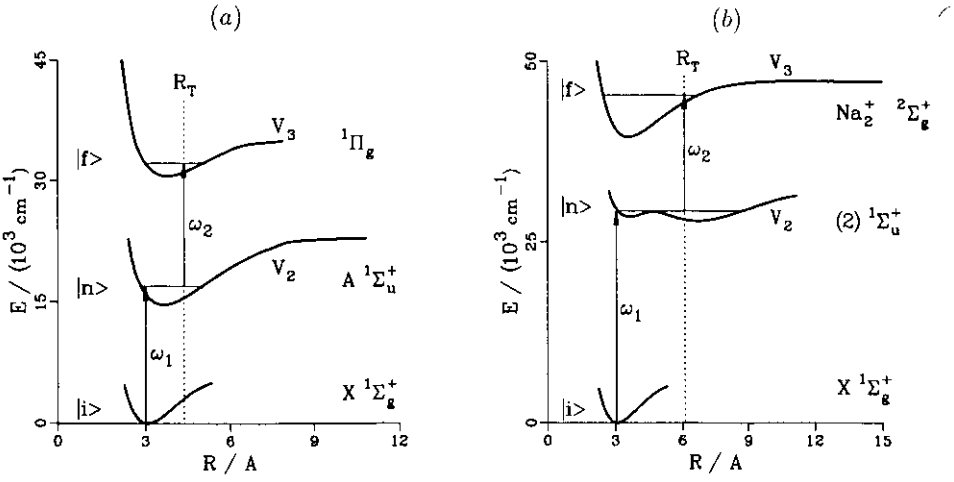

Figure 1. Laser-induced excitation processes of Na_2 studied in section 3.

In order to put the problem into perspective we study laser-induced excitation processes as shown in figure 1. A first short laser pulse (slowly varying pulse envelope $\mathcal{E}_1(t)$ centred around time t_1, pulse duration τ_1, frequency ω_1, polarization e_1) excites a coherent superposition of a large number of vibrational states $|n\rangle$ of a diatomic molecule starting from an energetically low lying vibrational state $|i\rangle$. Thus a vibrational wave packet is generated which represents a molecular quantum state where at each time the internuclear distance is well localized with respect to the size of the corresponding classically accessible region. The time evolution of this wave packet under the influence of the potential V_2 of the excited electronic state may

be probed with the help of a second short laser pulse (slowly varying pulse envelope $\mathcal{E}_2(t)$ centred around time t_2, pulse duration τ_2, frequency ω_2, polarization e_2) which induces a transition to some final state $|f\rangle$ after a time delay $\Delta t = t_2 - t_1$. Monitoring the final state probability as a function of the time delay Δt yields information about the dynamics of the vibrational wave packet. If both laser pulses are so weak that this two-photon excitation process can be described by time-dependent perturbation theory, long after the interaction with both laser pulses the final-state probability is given by

$$P_{i\to f} = |\langle 3, v_f|\psi\rangle_{t\to\infty}|^2$$
$$= |d_{23}d_{12}\int_{-\infty}^{\infty} \mathrm{d}\epsilon\ \mathrm{e}^{-\mathrm{i}\epsilon(t_2-t_1)}\langle v_f|[\epsilon - H_2 + \mathrm{i}0]^{-1}|v_i\rangle$$
$$\times\ \tilde{\mathcal{E}}_2(\epsilon + \omega_2 - \epsilon_f)\tilde{\mathcal{E}}_1(\epsilon_i + \omega_1 - \epsilon)|^2 \tag{1}$$

in the dipole and rotating wave approximation. (We use Hartree atomic units.) The initial and final vibrational states with energies ϵ_i and ϵ_f are denoted $|v_i\rangle$ and $|v_f\rangle$ and $\tilde{\mathcal{E}}_i(\Delta) = (1/\sqrt{2\pi})\int_{-\infty}^{\infty} \mathrm{d}t\ \mathcal{E}_i(t)\mathrm{e}^{-\mathrm{i}\Delta(t-t_i)}$ are the Fourier transforms of (the slowly varying envelopes of) pump (i=1) and probe (i=2) pulse. The electronic transitions $1 \to 2$ and $2 \to 3$ are described by the dipole matrix elements d_{12}, d_{23}, which also contain the contribution of the nuclear rotation and are assumed independent of R. The dynamics of the molecular vibrations in the excited electronic potential V_2 is described by the Hamiltonian $H_2 = -(1/2\mu)\mathrm{d}^2/\mathrm{d}R^2 + V_2(R)$. Since the reduced mass μ is large, effects of the nuclear rotation on H_2 may be neglected.

The quantity of central interest in equation (1) is the resolvent $[\epsilon - H_2 + \mathrm{i}0]^{-1}$ or equivalently the Green function

$$G_\epsilon(R, R') = \langle R|[\epsilon - H_2 + \mathrm{i}0]^{-1}|R'\rangle$$

which characterizes the dynamics of the molecular vibrations in the excited electronic potential V_2. In the simple one-dimensional case we are considering here, this Green function is given by

$$G_\epsilon(R, R') = \frac{2\mu}{W(f_\epsilon, g_\epsilon)} f_\epsilon(R_<)g_\epsilon(R_>) \tag{2}$$

with the Wronskian $W(f,g) = (f\mathrm{d}g/\mathrm{d}R - g\mathrm{d}f/\mathrm{d}R)$ and $R_< = \min\{R, R'\}$, $R_> = \max\{R, R'\}$. The two solutions of the homogeneous Schrödinger equation $f_\epsilon(R)$ and $g_\epsilon(R)$ fulfill the boundary conditions $f_\epsilon(R \to 0) = 0$ and $g_\epsilon(R \to \infty) = 0$. The reduced mass of a molecule is much larger than the electron mass so that the relevant classical actions are expected to be large and to a good approximation the Green function may be evaluated semiclassically. With the help of semiclassical approximations for $f_\epsilon(R)$ and $g_\epsilon(R)$ [5,6] the semiclassical Green function of a double minimum potential is given by

$$G_\epsilon(R, R') = (-2\mathrm{i}\pi)f_\epsilon(R_<)g_\epsilon(R_>)\sqrt{1-\rho^2}\,\mathrm{e}^{\mathrm{i}(S_1+S_2-\pi/2)}[1 - \rho\mathrm{e}^{2\mathrm{i}(S_1-\pi/2)}]^{-1}$$
$$\times \left[1 - \mathrm{e}^{2\mathrm{i}(S_2-\pi/2)}\frac{\rho - \mathrm{e}^{2\mathrm{i}(S_1-\pi/2)}}{1 - \rho\mathrm{e}^{2\mathrm{i}(S_1-\pi/2)}}\right]^{-1}. \tag{3}$$

Effects of the potential barrier are described by the (real valued) reflection coefficient $\rho = e^{-\tau}/\sqrt{1+e^{-2\tau}}$, the phase shift $\Phi = \arg\Gamma(\frac{1}{2}+i\tau/\pi) - (\tau/\pi)\ln|\tau/\pi| + \tau/\pi$ and the tunnelling integral

$$\tau = \begin{cases} -\int_{R_1^>}^{R_2^<} dR\ |k(R)| & (\epsilon \leqslant V_{max}) \\ -i\int_{R_+}^{R_-} dR\ k(R) & (\epsilon > V_{max}) \end{cases}$$

with the local momentum $k(R) = \sqrt{2\mu[\epsilon - V_2(R)]}$ and the turning points $R_1^>$, $R_2^<$ (real) and R_+, R_- (complex). Well below the potential barrier we typically have $\tau \to -\infty$ and therefore $\rho \to 1$, $\Phi \to 0$ whereas well above the barrier both the reflection coefficient and the phase shift tend to zero so that equation (3) reduces formally to the semiclassical Green function of a single-minimum potential with two turning points only. The (modified) classical actions $S_i = \int_{R_i^<}^{R_i^>} dR\ k(R) - \Phi/2$ $(i = 1,2)$ characterize the dynamics inside the corresponding potential wells and take account of barrier effects via the phase shift Φ (see figure 2(*a*)).

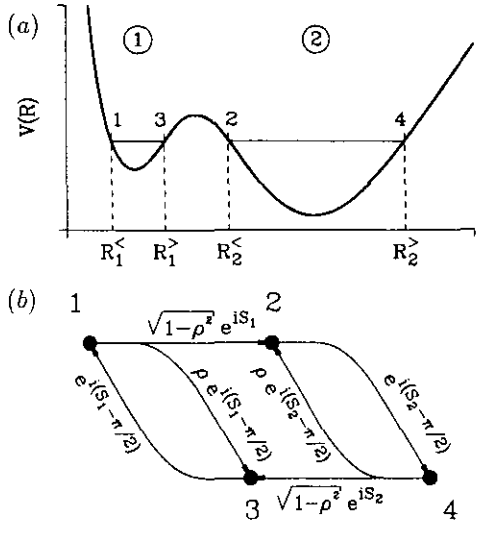

Figure 2. Double-minimum potential (*a*) and associated weighted graph G (*b*). The probability amplitudes which appear as matrix elements of the adjacency matrix are indicated on top of the corresponding edges of the graph.

For the solutions of the Schrödinger equation $f_\epsilon(R)$ and $g_\epsilon(R)$ simple uniform semiclassical approximations which are valid for all values of the internuclear distance R are not available. However, in the following we are mainly interested in cases where $R \ll R_1^>$ and $R_2^< \ll R'$. For these values of the internuclear distances uniform approximations are given by [5,6]

$$f_\epsilon(R) = \sqrt{\frac{2\mu}{\pi}}\sqrt{\pi}\left\{\frac{[3S(R_1^<, R)/2]^{2/3}}{k^2(R)}\right\}^{1/4} \mathrm{Ai}\{-[3S(R_1^<, R)/2]^{2/3}\} \qquad (4a)$$

$$g_\epsilon(R) = \sqrt{\frac{2\mu}{\pi}}\sqrt{\pi}\left\{\frac{[3S(R_2^>, R)/2]^{2/3}}{k^2(R)}\right\}^{1/4} \mathrm{Ai}\{[3S(R_2^>, R)/2]^{2/3}\} \tag{4b}$$

with the classical actions $S(R_{1(2)}^{<(>)}, R) = \int_{R_{1(2)}^{<(>)}}^{R} \mathrm{d}R'\ k(R')$ and the (regular) Airy-function $\mathrm{Ai}(x)$ [7].

Inserting the Green function of (3) into (1) and performing the energy integration with the help of the residuum theorem we would obtain the two-photon transition probability as a sum of contributions of all excited quantum states (*spectral or energy-eigenstate representation*) [3,8]. However, in describing the dynamics of a vibrational wave packet it is much more convenient to derive a *semiclassical path representation* for this observable. For this purpose we expand the denominators of equation (3) into geometric series thus obtaining

$$G_\epsilon(R, R') = (-2\mathrm{i}\pi) f_\epsilon(R_<) g_\epsilon(R_>) \times \sum_{L=j_0+j_1+\cdots=0}^{\infty} \frac{(j_1 + j_2 + \ldots)!}{j_1! j_2! \ldots} a_1^{j_0} a_2 a_3^{j_1} \prod_{s=0}^{\infty} (a_2^2 a_1^s)^{j_{s+2}} \tag{5}$$

with the probability amplitudes $a_1 = \rho \mathrm{e}^{2\mathrm{i}(S_1 - \pi/2)}$, $a_2 = \sqrt{1-\rho^2}\mathrm{e}^{\mathrm{i}(S_1+S_2-\pi/2)}$ and $a_3 = \rho \mathrm{e}^{2\mathrm{i}(S_2-\pi/2)}$. Now the semiclassical Green function is expressed as a sum of contributions of all classical and non-classical (tunnelling) paths which lead from point R to point R'. Thereby effects due to tunnelling and above-barrier reflection are fully taken into account.

With the help of the graph-theoretical concept of a weighted graph and its associated adjacency matrix this Green function may be written in a particularly concise form. For this purpose we introduce the graph G which is shown in figure 2(*b*). Its vertices represent the four (real or complex valued) turning points of the double-minimum potential. The (directed) edges of the graph represent simple paths which connect these turning points. A general path of this graph is defined as an arbitrary sequence of directed edges. This way each summand of the semiclassical path representation of equation (5) corresponds in a unique way to the contribution of a path of the graph G. With this graph we associate a (weighted) *adjacency matrix* $\mathcal{A}$. In our case this is a 4×4 matrix whose matrix elements are zero if the corresponding vertices of the graph G are not connected and whose non-zero matrix elements are given by the probability amplitude associated with the simple path connecting the corresponding vertices. Thus, for example, the matrix element $\mathcal{A}_{12}$ equals the probability amplitude of the path which connects turning points 1 and 2 of the double-minimum potential (see figure 2). Furthermore, the matrix element

$$(\mathcal{A}^m)_{ij} = \sum_{n_1,\ldots,n_{m-1}=1}^{4} \mathcal{A}_{in_1}\mathcal{A}_{n_1n_2}\cdots\mathcal{A}_{n_{m-1}j}$$

is the sum of the probability amplitudes of all paths of 'length m' which consist of m directed edges and connect points i and j. If we choose the adjacency matrix in the form

$$\mathcal{A} = \begin{pmatrix} 0 & \sqrt{1-\rho^2}\mathrm{e}^{\mathrm{i}S_1} & \rho\mathrm{e}^{-\mathrm{i}\pi/2}\mathrm{e}^{\mathrm{i}S_1} & 0 \\ 0 & 0 & 0 & \mathrm{e}^{-\mathrm{i}\pi/2}\mathrm{e}^{\mathrm{i}S_2} \\ \mathrm{e}^{-\mathrm{i}\pi/2}\mathrm{e}^{\mathrm{i}S_1} & 0 & 0 & 0 \\ 0 & \rho\mathrm{e}^{-\mathrm{i}\pi/2}\mathrm{e}^{\mathrm{i}S_2} & \sqrt{1-\rho^2}\mathrm{e}^{\mathrm{i}S_2} & 0 \end{pmatrix}$$

the semiclassical path representation of equation (5) may be written in the more concise form

$$G_\epsilon(R,R') = (-2i\pi) f_\epsilon(R_<) g_\epsilon(R_>) \{[1-\mathcal{A}]^{-1}\}_{14}$$
$$= (-2i\pi) f_\epsilon(R_<) g_\epsilon(R_>) \sum_{m=0}^{\infty} \{\mathcal{A}^m\}_{14} \tag{6}$$

with $(\mathcal{A}^m)_{14}$ being the probability amplitude associated with all classical and non-classical paths of 'length' m which connect turning points 1 and 4. Equations (5) and (6) are the main results of this paper. Using the same type of approach, recently a semiclassical path representation for the energy-dependent Green function of a general multiple-well potential has been derived also [9].

With the help of the semiclassical Green function of (3) and (6) we can easily derive semiclassical approximations for the two-photon transition amplitude which describe a laser-induced pump–probe process with two time-delayed short laser pulses. According to equation (1) for this purpose we have to evaluate the matrix elements $\langle v_f|[\epsilon - H_2 + i0]^{-1}|v_i\rangle = \int_0^\infty dR \int_0^\infty dR'\ v_f^*(R) G_\epsilon(R,R') v_i(R')$ of the Green function. In the following we are mainly interested in cases where the initial vibrational state $|v_i\rangle$ is an energetically low-lying (well localized) vibrational state whereas the final vibrational state $|v_f\rangle$ is highly excited and delocalized. This implies that the absorption of the first laser photon is essentially localized around the leftmost turning point of the excited vibrational states of potential V_2 and that according to the Franck–Condon principle the absorption of the second laser photon takes place around the internuclear distance R_T at which $V_3(R_T) - V_2(R_T) = \omega_2$. If the transition point R_T is located on the right hand side of the potential barrier, i.e. $R_T > R_2^<$, the integration over R' may be achieved with the help of uniform approximations. Using (4) and (6) we find in the case of $\Delta S_{32}'' < 0$

$$\langle v_f|[\epsilon - H_2 + i0]^{-1}|v_i\rangle = (-2i\pi)[1-\mathcal{A}]_{14}^{-1} \langle f_\epsilon|v_i\rangle (-1)^{n_f} \frac{\mu}{\pi} \sqrt{\frac{2\pi}{T_f}}$$
$$\times |k_2(R)|^{-1} \sqrt{\frac{2\pi^2}{|\Delta S_{32}''|}} |\tfrac{3}{2}\Delta S_{32}|^{1/6} \mathrm{Ai}[-(\tfrac{3}{2}\Delta S_{32})^{2/3}]|_{R=R_T} \tag{7}$$

with the classical vibration time in the final electronic potential T_f and the difference between the classical actions in potentials V_3 and V_2 denoted $\Delta S_{32} = S_3(R, R_f^>) - S_2(R, R_2^>)$. Inserting this expression into equation (1) we obtain the semiclassical path representation of the two-photon transition amplitude for cases where the second laser photon is absorbed in the second potential well. Considered as a function of the time delay Δt between both laser pulses this transition probability will be large whenever Δt equals the time the vibrational wave packet takes to evolve from the initial excitation point at $R \approx R_1^<$ to the final transition point R_T along any of the paths of the graph G.

3. Applications

In this section we discuss the dynamics of vibrational wave packets in single-minimum and double-minimum electronic potentials of Na_2. Based on the semiclassical path

representation of the Green function as given in (6) we derive simple analytical expressions for the two-photon excitation probability which is measured in typical pump–probe experiments with weak laser pulses.

In general, no simple analytical expressions are available for the two-photon transition probability and the integration over energy in (1) has to be performed numerically. However, depending on the position of the transition point with respect to the turning points of the potential, for laser pulses with Gaussian pulse shapes, i.e. $\mathcal{E}_i(t) = \mathcal{E}_i e^{-(t-t_i)^2/(4\tau_i^2)}$ $(i = 1,2)$, simple analytical expressions may be derived. In the following we discuss two such cases in more detail, namely the cases where the transition point is in the classically allowed region or at the turning point. Thereby we assume for simplicity that the first short laser pulse generates a vibrational wave packet close to the leftmost turning point of the excited electronic potential V_2 (see figure 1) where the potential is assumed to be so steep that $|\sigma\, V_2'(R_1^<)| \gg \Delta\epsilon = [\tau_1^2+\tau_2^2]^{-1/2}$, where σ indicates the extension of the initial state $|v_i\rangle$. Then the Franck–Condon factor $\langle f_\epsilon|v_i\rangle$ is approximately energy independent over the significantly excited energy range $\Delta\epsilon$ of excited energies. This range is determined by the pulse durations τ_1 and τ_2.

3.1. Transition point in the classically allowed region

The simplest situation arises if the transition point R_T is located in the classically allowed regions of potentials V_2 and V_3. In this case the corresponding Franck–Condon factor may be evaluated with the help of primitive semiclassical approximations. In particular, in cases where this transition point is located in the second potential well, the primitive semiclassical approximation for the relevant matrix elements of the Green function may be obtained from the uniform expression as given in (7). This is done by taking into account the fact that $\Delta S_{32} \gg 1$ and replacing the Airy function by its asymptotic expression. With the additional assumptions that

(i) the reflection coefficient ρ is approximately energy independent over the excited energy range $\Delta\epsilon$ and that

(ii) the anharmonicity of the electronic potential V_2 is sufficiently small so that all classical actions appearing in (1) may be expanded up to second order with respect to energy,

equation (1) reduces to an energy integral over Gaussian functions. Thus we find

$$
\begin{aligned}
P_{i\to f} = P_0 \Big| < f_\epsilon|v_i > \frac{\mu}{\pi}\sqrt{\frac{2\pi}{T_f}}|k_2(R_T)|^{-1}\sqrt{\frac{2\pi}{|\Delta S_{32}''|}}
\\
\times \sum_{\gamma(1\to 4)} (\sqrt{1-\rho^2})^{t_\gamma}(\rho e^{-i\pi/2})^{r_\gamma} e^{i[n_\gamma^{(1)}S_1 + n_\gamma^{(2)}S_2]} e^{-i m_\gamma \pi/2}
\\
\times \Big\{ \exp[i(\Delta S_{32} + \pi/4)]\sqrt{\frac{\pi}{[\tau_\gamma^+]^2}}\exp\{-[\Delta t - T_\gamma + T_{4\to R_T}]^2/[2\tau_\gamma^+]^2\}
\\
- \exp[-i(\Delta S_{32} + \pi/4)]\sqrt{\frac{\pi}{[\tau_\gamma^-]^2}}
\\
\times \exp\{-[\Delta t - T_\gamma - T_{4\to R_T}]^2/[2\tau_\gamma^-]^2\}\Big\}\Big|^2_{\epsilon=\bar\epsilon}
\end{aligned}
\tag{8}
$$

with $P_0 = |2\pi(d_{12}\mathcal{E}_1\tau_1)(d_{23}\mathcal{E}_2\tau_2)|^2$ and the mean excited energy $\bar{\epsilon} = \epsilon_i + \omega_1 = \epsilon_f - \omega_2$. The index $\gamma(1 \to 4)$ indicates all possible paths of the graph G which connect turning points 1 and 4. The integers t_γ, r_γ, $n_\gamma^{(1)}$, $n_\gamma^{(2)}$ and m_γ are equal to the number of transmissions (t) and reflections (r) at the barrier, to the number of vibrations in the first ($n^{(1)}$) and second ($n^{(2)}$) potential well and to the number of reflections at turning points 1 and 4 (m) along path γ. The time for propagation from turning point 1 to 4 along path γ is given by $T_\gamma = \mathrm{d}(n_\gamma^{(1)}S_1 + n_\gamma^{(2)}S_2)/\mathrm{d}\epsilon$ and $T_{4\to R_T}$ is the time for propagation from turning point 4 to the transition point R_T. We should point out that, because of the energy dependence of the phase shift Φ which originates from the potential barrier, the quantity T_γ reduces to its classical value only well above the barrier. Close to the barrier its value remains finite, contrary to the corresponding classical value which tends to infinity at the barrier.

According to (8) a peak appears in the two-photon transition probability whenever the time delay between pump and probe pulse Δt equals the time it takes for a transmitted fraction of the wave packet to move from the initial excitation point (turning point 1) to the transition point R_T. The quantities

$$\begin{aligned}[\tau_\gamma^+]^2 &= \tau_1^2 + \tau_2^2 - \tfrac{1}{2}\mathrm{i}[T'_\gamma - T'_{4\to R_T}] \\ [\tau_\gamma^-]^2 &= \tau_1^2 + \tau_2^2 - \tfrac{1}{2}\mathrm{i}[T'_\gamma + T'_{4\to R_T}]\end{aligned} \tag{9}$$

determine the widths of the corresponding contributions with the + and − signs distinguishing contributions where the transition point is reached with positive or negative momentum. The primes indicate derivatives with respect to energy. For mean excited energies well above the potential barrier we have $\Phi, \rho \to 0$ and formally (8) reduces to the result we would obtain for motion in a single-minimum potential with two turning points only.

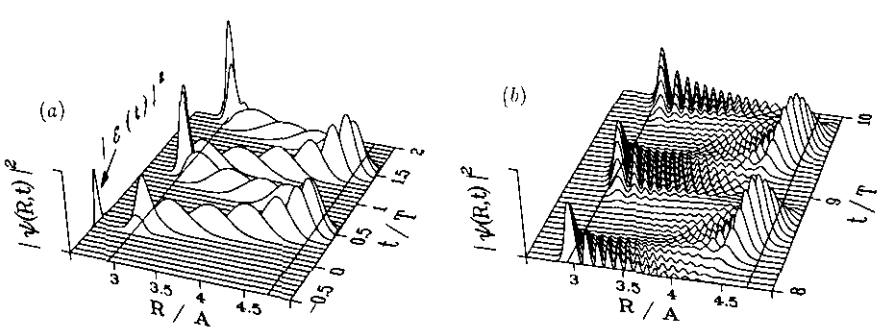

Figure 3. Time evolution of a vibrational wave packet in the $A\,^1\Sigma_u^+$ potential of Na_2 (see figure 1(*a*)): $\tau_1 = 10$ fs ($T = 310$ fs is the mean classical vibration time).

Figure 3 shows the time evolution of a vibrational wave packet which is generated in the $A\,^1\Sigma_u^+$ electronic potential of Na_2 by a short laser pulse near the left turning point (see figure 1(*a*)). The time evolution of the wave packet has been calculated numerically. Figure 4 shows the corresponding time dependence of the two-photon transition probability. The full curve shows the result of a numerical computation of the two-photon transition probability based on a summation over all excited energy

eigenstates and the dashed curve shows the corresponding result obtained from equation (8) in the limit of a single-minimum potential. With the help of equation (8) the various peaks of figure 4 may be interpreted in terms of probability amplitudes of paths leading from the initial excitation point (turning point 1) to the transition point R_T. With each return of the vibrational wave packet to the transition point the second laser pulse may induce a transition to the final state. Typically, contributions associated with successive returns to the transition point show a doublet structure because the transition point may be reached with positive or negative momentum. According to figure 4, with increasing time delay Δt contributions originating from paths which reach the transition point with positive momenta are broadened much faster than the corresponding contributions from negative momenta. This is due to the negative sign of the quantity $T'_{4\rightarrow R_T}$ which describes a narrowing of the wave packet on its way from turning point 4 to the transition point R_T. According to (8) and (9) this narrowing of the wave packet leads to a narrowing of the corresponding peaks of the two-photon transition probability until a minimum width is reached when the contributing path becomes so long that $T'_\gamma \geqslant |T'_{4\rightarrow R_T}|$.

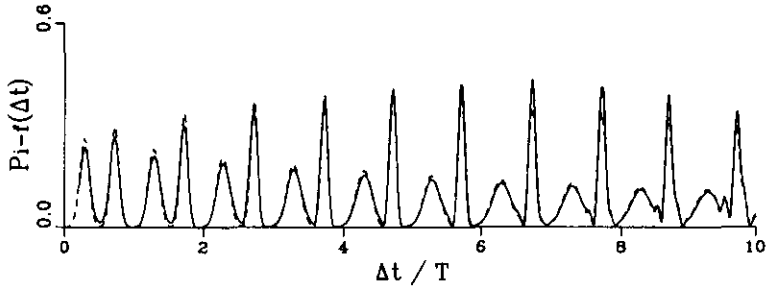

Figure 4. Two-photon transition probability of the wave packet of figure 3 as a function of the time delay Δt between pump and probe pulse ($\mathcal{E}_1 = \mathcal{E}_2$, $\tau_1 = \tau_2 = 10$ fs); numerical evaluation (full curve), equation (8) (dashed curve). The transition point R_T is located in the classically allowed region (see figure 1 (*a*)).

We remark that, even in cases where the Fourier transform of the energy-dependent Green function of equation (1) has to be determined numerically, the semiclassical path representation of the Green function as given in equation (6) offers a valuable tool for interpreting pump–probe experiments. As an example let us consider the generation of a vibrational wave packet in a double-minimum potential in the energy range around the potential barrier. Figure 5 shows the two-photon transition probability of a vibrational wave packet which has been generated by a short laser pulse at the leftmost turning point of the $(2)^1\Sigma_u^+$ potential of Na_2 (figure 1(*b*)). In this example the pulse durations of pump and probe pulse are so short that the reflection coefficient of the potential barrier ρ cannot be considered constant over the excited energy range and the Fourier transform of equation (1) has to be evaluated numerically. In particular, in figure 5(*c*) the numerical evaluation of the two-photon transition probability based on a summation over all excited energy eigenstates (full curve) is compared with an evaluation based on the semiclassical path representation of equation (6) (R_T in the classically accessible region, dashed curve). As a large number of energy eigenstates are excited coherently by the first short laser pulse a direct interpretation of figure 5(*c*) based on a summation over excited energy eigenstates is difficult. With the help of the semiclassical path representation each peak of figure 5(*c*) may be associated with a coherent sum of probability amplitudes

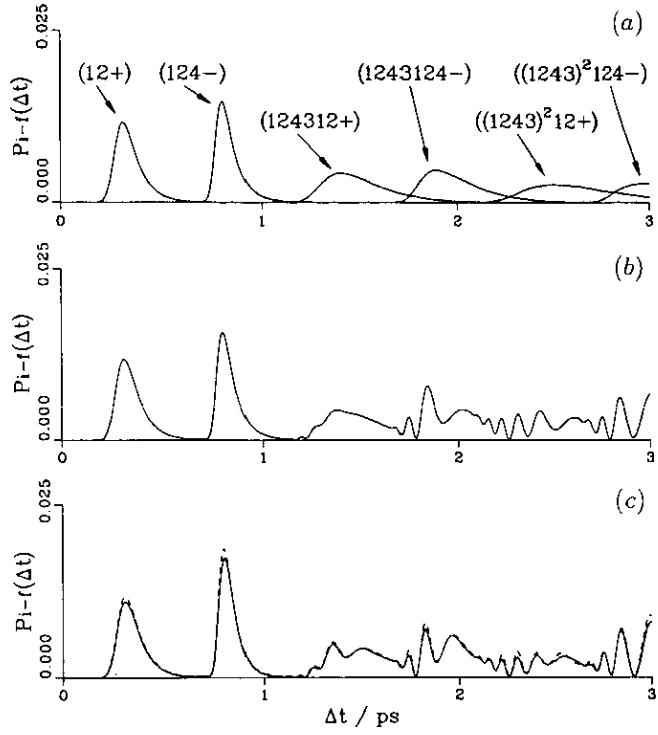

Figure 5. Two-photon transition probability for a vibrational wave packet which is generated in the $(2)^1\Sigma_u^+$-double-minimum potential of Na_2 (see figure 1(*b*)) in the energy region around the potential barrier ($\mathcal{E}_1 = \mathcal{E}_2$, $\tau_1 = \tau_2 = 10$ fs). (*a*) Transition probabilities of single paths with quantum mechanical interferences neglected. The paths are indicated on top of the corresponding peaks (see figure 2(*b*). The + and − signs indicate whether the transition point is reached with positive or negative momentum. (*b*) As (*a*) but with quantum mechanical interferences taken into account. (*c*) Numerical (full curve) and semiclassical path result (dashed curve). In the semiclassical result the 60 shortest semiclassical paths have been taken into account.

associated with only a few paths of the graph G which start from the excitation point of the wave packet, i.e. turning point 1, and reach the transition point R_T after time Δt. In this example the transition point is located in the classically accessible region of the second potential well. Therefore any path reaching the transition point has been transmitted by the potential barrier. Figure 5(*a*) shows the probabilities of a few short paths which have not been reflected by the potential barrier on their way to the transition point. Figure 5(*b*) shows the corresponding coherent sum of their probability amplitudes. Comparison with the numerical result of figure 5(*c*) shows that these purely transmitted paths yield the dominant contributions to the two-photon transition probability. The dashed curve in figure 5(*c*) shows a semiclassical path evaluation including the 60 shortest paths (taking into account also paths which have once been reflected at the potential barrier). Now even the fine details of the interferences which appear in the numerical result are reproduced. Besides the good quantitative agreement the semiclassical path representation also offers the advantage of a clear physical interpretation of the time dependence of pump–probe experiments in terms of probability amplitudes associated with classical and non-classical tunnelling paths

leading from the initial excitation point to the final transition point.

3.2. Transition point at turning point

With the help of uniform approximations for the relevant matrix elements of the Green function we may easily derive simple analytical expressions for the two-photon transition probability which are also valid if the transition point R_T is close to the turning points of the electronic potentials V_2 and V_3. In the case, for example, where this transition point is located close to the rightmost turning points of both excited electronic potentials we may use the uniform approximation given in equation (7). Linearizing the potentials around turning point $R_3^>$ and assuming

(i) Gaussian laser pulses,

(ii) an approximately energy independent reflection coefficient ρ and

(iii) weak anharmonicity of the excited electronic potential V_2

we find

$$P_{i\to f} = P_0 \left| 2\sqrt{\frac{2\pi}{T_f}} \langle f_\epsilon | v_i \rangle \right| 2\mu \frac{t_0}{V_3' \Delta V'} \Bigg|^{1/4}$$

$$\times \sum_{\gamma(1\to 4)} (\sqrt{1-\rho^2})^{t_\gamma} (\rho e^{-i\pi/2})^{r_\gamma} \exp\{i[n_\gamma^{(1)} S_1 + n_\gamma^{(2)} S_2]\} e^{-i m_\gamma \pi/2}$$

$$\sqrt{\frac{\pi}{\tau_\gamma^2}} \exp[\![-\{[\Delta t - T_\gamma]^2/[2\tau_\gamma]^2 + \tfrac{1}{3} t_0^6/[4\tau_\gamma^2]^3 + \beta t_0^2/[2\tau_\gamma]^2\}]\!]$$

$$\times \mathrm{Ai}(-\beta) \Big|^2_{\epsilon=\bar{\epsilon}}. \tag{10}$$

In (10) the difference potential is given by $\Delta V = V_3 - V_2$ and all potentials and their derivatives have to be evaluated at the right turning point of potential V_3, i.e. at $R_3^>$. Furthermore we have defined

$$\beta = t_0[\bar{\epsilon} - V_2] - \left[\frac{t_0^2}{4\tau_\gamma^2}\right]^2 - i t_0 [\Delta t - T_\gamma]/[2\tau_\gamma^2]$$

$$t_0 = \mathrm{sgn}(\Delta V') \left| 2\mu \frac{V_3'}{\Delta V' (V_2')^2} \right|^{1/3}$$

$$\tau_\gamma^2 = \tau_1^2 + \tau_2^2 - \tfrac{1}{2} i T_\gamma'.$$

Figure 6 shows the two-photon transition probability for the vibrational wave packet of figure 3 in the single-minimum potential. The transition point is close to the right turning point of potentials V_2 and V_3. The full curve in figure 6 shows the result of a numerical calculation which is based on an energy-eigenstate representation of the two-photon transition probability. The almost indistinguishable dashed curve shows the corresponding result using equation (10) (with $\rho \boxminus 0$).

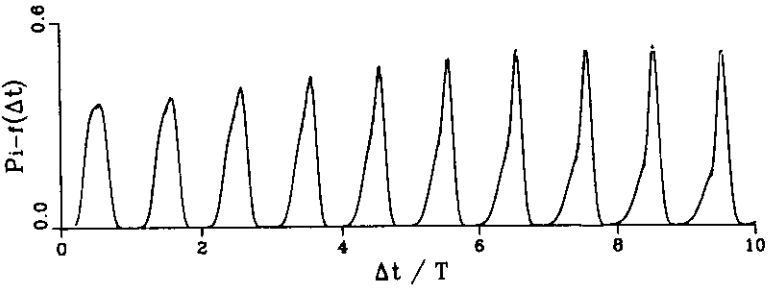

Figure 6. As figure 4 but with transition point at the right turning point of potential V_2 ($\bar{\epsilon} = V_2(R_3^>)$); numerical evaluation (full curve), equation (10) (dashed curve).

4. Summary

With the help of graph-theoretical concepts we have presented a semiclassical path representation of the energy-dependent Green function which describes the quantum dynamics of a particle in a double-minimum potential. Using uniform semiclassical methods, effects of tunnelling and above-barrier reflection have been taken into account. By focusing on two-photon transition probabilities, which are of interest for time-resolved studies of the dynamics of vibrational molecular wave packets in Na_2, we have shown that these semiclassical path representations yield good quantitative results and clearly exhibit the connection between the quantum dynamics of a wave packet and the corresponding classical dynamics of a particle.

Acknowledgment

This work was supported by Sonderforschungsbereich 276 of the Deutsche Forschungsgemeinschaft.

References

[1] Khundkar L R and Zewail A H 1990 *Ann. Rev. Phys. Chem.* **41** 15
[2] Engel V 1991 *Comput. Phys. Commun.* **63** 228
[3] Strunz W, Alber G and Briggs J S 1990 *J. Phys. B: At. Mol. Opt. Phys.* **23** L697
[4] Baumert T, Bühler B, Grosser M, Thalweiser R, Weiss V, Wiedenmann E and Gerber G 1991 *J. Chem. Phys.* at press
[5] Berry M V and Mount K E 1972 *Rep. Prog. Phys.* **35** 315
[6] Child M S 1980 *Semiclassical Methods in Molecular Scattering and Spectroscopy* ed M S Child (Dordrecht: Reidel) p 127
[7] Abramowitz M and Stegun I (ed) 1964 *Handbook of Mathematical Functions (NBS Appl. Math. Ser. 55)* (Washington, DC: US Government Printing Office)
[8] Alber G and Zoller P 1991 *Phys. Rep.* **199** 231
[9] Strunz W T 1992 *J. Phys. A: Math. Gen.* submitted